

# Spreading change of Africa–South America plate: insights from space geodetic observations

Shuanggen Jin · J. Wang

Received: 27 April 2004 / Accepted: 23 May 2007 / Published online: 12 July 2007  
© Springer-Verlag 2007

**Abstract** The results derived from geological data show that the half-spreading rate between the African and South American plates has remained relatively constant at 2 cm/year over the past 80 million years (Silver et al. in *Science* 279:60–63, 1998). In this paper, we have reestimated a new relative angular velocity of Africa–South America plates using the selected space geodetic station data through a new method. Our angular velocity estimates the spreading rates of Africa–South America plate over several years that are similar in azimuth but significantly slower in rate than the NUVEL-1A predictions averaged over the past 3 million years. The implied rates of deceleration coincide with longer-term trends over the past 35 million years and may reflect the effects of plate interaction and coupling of Africa–South America plates.

**Keywords** Plate motion · Space geodesy · African plate · South American plate

## Introduction

The magnitude to which plates can change their motions over brief geological intervals is a key unanswered question in the studies of plate kinematics, which has important

implications for the forces that drive plate motion. The advent of space geodetic techniques, especially the global positioning system (GPS), provide an important tool for directly studying the current motions of plates (Gordon and Stein 1992; Jin and Zhu 2003a). Comparing space geodetic measurements of plate velocities over a few years with NUVEL-1A estimations averaged over the past 3 million years (DeMets et al. 1990, 1994) will enable future tests for geologically recent changes in the velocities of the tectonic plate motions (e.g. Africa–South America plates). Silver et al. (1998) have analyzed the motion histories of Africa–South America plate over the past 80 million years using fracture-zone orientations, sea-floor magnetic anomalies and hot spot data, and found that the half-spreading rate between the Africa and South America plates remained relatively constant at 2 cm/year. However, the recent changes of the Africa–South America plate remain indistinct due to the lack of space geodetic observations or short observation histories for only a few stations in Africa. For instance, there is only one core site locating at the plate boundary in the African plate employed by the ITRF2000 (International Terrestrial Reference Frame, 2000), so Altamimi et al. (2002) did not directly calculate the angular velocity of the African plate. Here we used more space geodetic stations in the African plate from Fernandes et al. (2003, 2004) incorporating the ITRF2000 velocity field. These space geodetic data are essential for an improved estimate of the relative motion between the African and South American plates.

The selection of sites to define the angular velocities of plates is very important. In ITRF2000 (<http://www.lareg.ensg.ign.fr/ITRF/ITRF2000/>), the criteria for selecting core sites are: (a) continuously observed with at least 3 years; (b) located far away from plate boundaries and deforming zones; (c) velocity accuracy better than

---

S.G. Jin (✉)  
Space Geodesy Research Group,  
Korea Astronomy and Space Science Institute,  
Daejeon 305-348, South Korea  
e-mail: sgjin@kasi.re.kr; sg.jin@yahoo.com

S.G. Jin · J. Wang  
School of Surveying and Spatial Information Systems,  
The University of New South Wales,  
Sydney, NSW 2052, Australia

3 mm/year and (d) velocity residuals less than 3 mm/year for at least three different solutions. However, the core sites constrained on the ITRF2000 with space geodetic techniques are chosen with some randomness and uncertainties. For instance, such criteria are not clearly defined: (a) how far the sites are from the plate boundary or deformation zones; (b) what residual and velocity accuracies of the sites are optimal (e.g. better than 3 or 2 mm/year).

Sella et al. (2002) selected space geodetic stations located in the areas more than 100 km away from the nearest plate boundary to define the angular velocities of the plate. Heki (1996) selected permanent VLBI stations located in the areas more than 500 km away from the nearest plate boundary to define the kinematics reference frame. Fernandes et al. (2003) and Jin et al. (2002, 2003b) selected geodetic stations with a formal uncertainty for their 3D velocity smaller than 10 and 5 mm/year, respectively, to define the Euler rotation parameter of the plate, and so on. Comparing the geodetic results with the NNR-NUVEL-1 model (Argus and Gordon 1991; DeMets et al. 1994; Jin and Zhu 2004), the most obvious discrepancy is the angular velocity of the South American plate calculated by Sillard et al. (1998) due to the inappropriate selection of geodetic sites on the plate. Therefore, the criteria of site selection directly affect the precision and reliability of the plate motion angular velocity.

In this paper, we present a new method to select rigid geodetic sites on the plate from the ITRF2000 velocity field and regional GPS solutions from Fernandes et al. (2003 and 2004). The relative angular velocity of Africa–South America plate is obtained from the selected sites, and further used to accurately estimate the present-day spreading velocities of Africa–South America plate and discuss motion trends and implications for our understanding of spreading at the South mid-Atlantic Ridge.

## Site selection on the plates

### Selection method

At present, the horizontal velocity accuracy of space geodetic techniques is about 1–2 mm/year, which is sufficient for us to monitor the crustal deformation and plate motions in the horizontal direction at about a cm/year level. The vertical accuracy of space geodetic techniques, however, is relatively lower (about 2–5 mm/year), it is difficult to detect the vertical variations with a magnitude of several mm/year. For instance, the continuous GPS data of Shanghai IGS station collected from 1998 to 2003 was processed, and the vertical velocity of Shanghai GPS station was shown to be  $-1.9 \pm 0.6$  mm/year. If the Shanghai GPS data collected from 1995 to 2003 is processed, the vertical velocity is

$+1.5 \pm 0.4$  mm/year (Jin 2003c). Such discrepancy will affect crustal deformation and plate rigidity analysis. In addition, unification and transformation of geodetic solutions in different reference frames are normally realized in the three dimensions (East, North and Vertical) with the well-known 14 transformation parameters, such as between the ITRF2000 solutions and regional IGS analysis center solutions. The bad vertical velocity will inevitably affect the final unification solutions. Therefore, the involved vertical velocity may degrade the residual analysis and rigidity study of plate motion. However, ones used 3D velocity field to study on the plate rigidity in the past. For example, Li et al. (2001) identified the rigid VLBI sites on the plate by analyzing the three dimension deformational residuals, etc.

Here, let the geodetic horizontal velocity be expressed as

$$v_{ij} = v_{ij}^r + v_{ij}^d + v_{ij}^i + \varepsilon_{ij}, \quad (1)$$

where  $v_{ij}$  is the horizontal velocity of geodetic measurement in the  $i$ th station of the  $j$ th plate,  $v_{ij}^r$ ,  $v_{ij}^d$ ,  $v_{ij}^i$  and  $\varepsilon_{ij}$  are the horizontal velocity caused by the rigid plate motion, local deformation, postglacial rebound, and observation noise, respectively. The  $v_{ij}^r$  can be written as

$$v_{ij}^r = v_{ij}^m + (\vec{\Omega} \times \vec{r}_i)_h, \quad (2)$$

where  $v_{ij}^m$  is the prediction from plate motion model,  $r_{ij}$  is the position vector in the  $i$ th station of the  $j$ th plate, and  $(\vec{\Omega} \times \vec{r}_i)_h$ , the horizontal rate of Euler rotation motion, can be expressed as

$$\begin{aligned} (\vec{\Omega} \times \vec{r}_i)_h &= \begin{pmatrix} V_n \\ V_e \end{pmatrix} \\ &= \begin{pmatrix} R \sin \lambda_i & -R \cos \lambda_i & 0 \\ -R \sin \varphi_i \cos \lambda_i & -R \sin \varphi_i \sin \lambda_i & R \cos \varphi_i \end{pmatrix} \begin{pmatrix} \Omega_x \\ \Omega_y \\ \Omega_z \end{pmatrix} \end{aligned} \quad (3)$$

where  $\lambda_i$  and  $\varphi_i$  are the longitude and latitude of station  $i$ , respectively, and  $R$  is the radius of the Earth. So,  $v_{ij}$  can be written as

$$\begin{aligned} v_{ij} &= v_{ij}^m + v_{ij}^d + v_{ij}^i \\ &+ \begin{pmatrix} R \sin \lambda_i & -R \cos \lambda_i & 0 \\ -R \sin \varphi_i \cos \lambda_i & -R \sin \varphi_i \sin \lambda_i & R \cos \varphi_i \end{pmatrix} \\ &\times \begin{pmatrix} \Omega_x \\ \Omega_y \\ \Omega_z \end{pmatrix} + \varepsilon_{ij} \end{aligned} \quad (4)$$

The  $v_{ij}^m$  can be obtained from the NNR-NUVEL1A model (Argus and Gordon 1991; DeMets et al. 1994),  $v_{ij}^i$  can be

obtained from the postglacial rebound model ICE-4G, so these parameters are the known quantities,  $\Omega_x$ ,  $\Omega_y$  and  $\Omega_z$  are the unknown parameters; with adequate observations,  $\varepsilon_{ij}$  are assumed to obey the normal distribution. If the local deformation  $v_{ij}^d$  is ignored,  $v_{ij}$  can be written as

$$v_{ij} = v_{ij}^m + v_{ij}^i + A\Omega \quad (5)$$

where  $\Omega$  is the Euler's rotation parameters ( $\Omega_x, \Omega_y, \Omega_z$ )<sup>T</sup>,  $A$  is a matrix of coordinate coefficients. For the  $j$ th plate with more than two geodetic sites, the parameters  $\Omega$  can be estimated through a weighted least squares adjustment to all the stations on the  $j$ th plate, namely

$$\Omega = (A^T P A)^{-1} A^T P (v_{ij} - v_{ij}^m - v_{ij}^i) \quad (6)$$

Let  $v_{ij}^d$  be the post-fit residual that is regarded as a random series with a variance  $\sigma^2$ . We reject the stations with absolute values of  $v_{ij}^d$  larger than  $k\sigma$ . In order to choose an appropriate value  $k$ , let us classify all the stations on the  $j$ th plate into two groups. In Group 1, suppose only rigid plate stations are included, the corresponding variance of the post-fit residual series and the sum of weightings are  $\sigma_1$  and  $P_1$  respectively. In Group 2 only stations within deforming zones are included, the corresponding quantities are  $\sigma_2$  and  $P_2$ . Then the variance ( $\sigma$ ) of the post-fit residual series for all the stations on the  $j$ th plate can be expressed as

$$\sigma^2 = (\sigma_1^2 P_1 + \sigma_2^2 P_2) / (P_1 + P_2) \quad (7)$$

Because  $\sigma_1$  is smaller than  $\sigma_2$ , it is clear to see:  $\sigma_1 < \sigma < \sigma_2$ , so we adopt  $1\sigma$  as the criterion, namely  $k = 1$ .

Then we re-estimate the parameters ( $\Omega_x, \Omega_y, \Omega_z$ ) by using only those kept stations and repeat the above estimating and rejecting calculation until no sites are rejected, the estimation of the parameters and the variance of post-fit residuals are not changed significantly before and after the rejecting operation. The motions of the final remaining stations can be taken as the candidates of rigid sites.

### GPS velocity field

There are 18 GPS sites on the South American plate and 13 sites on the African plate (see Table 1). Velocity residuals of stations on the South American and African plates are shown in Figs. 1 and 2, respectively. Although we add the GPS station data on the African plate which are not available in ITRF2000, however, most GPS stations remain in the Nubian, and a few stations located in Somalia that are not good enough to abide with geological plate motions (Chu and Gordon 1999). Therefore the Africa is still regarded as a single plate (Fernandes et al. 2003). Using the site selection method outlined above, we carefully select

the stations on the African and South American plates. For instance, Table 2 shows the rejecting process of the sites for the South America plate. In Circle 1,  $\sigma$  was 5.8834 mm/year, eight stations with absolute values of  $v_{ij}^d$  larger than  $1\sigma$  (5.8834 mm/year), and the eight sites were rejected. In Circle 2,  $\sigma$  was dramatically decreased to 3.6503 mm/year, and three stations with absolute values of  $v_{ij}^d$  larger than  $1\sigma$  (3.6503 mm/year) were rejected. In Circle 3,  $\sigma$  was further decreased but only one site (RIOG) was rejected. In Circle 4, the site PARA was rejected. Till Circle 5, no sites were rejected, and the value of  $\sigma$  and the estimation to parameters were not changed significantly. Table 3 shows the five sites kept in Circle 5, and the absolute values of residuals for all the two components of velocity were less than 1.2910 mm/year. Using the same method, the four sites (MASP, GOUG, TGCV and SUTH) on the African plate were selected.

### Angular velocity of Africa–South America plate

The five selected sites on the South American plate contain the four core sites employed by the ITRF2000 for ITRF2000 orientation. Similarly, the selected sites on the African plate contain the core site MASP employed by the ITRF2000. In addition, the selected nine sites located on the African and South American plates all satisfy the rigid motion test (Argus and Gordon 1998). Although the GPS site ASC1 is located near the boundary between the South American and African plates, it is still a rigid site of the South America plate. Consequently, the selected five sites on the plate are consistent with the plate rigid motion.

In order to estimate the spreading motion of Africa–South America plate, the relative angular velocity of Africa–South America plate was accurately calculated through a weighted least-squares algorithm. Table 4 lists the relative angular velocities of Africa–South America plate.

### South America–Africa motion

We calculate and compare present-day spreading rates of Africa–South America plate using several angular velocities (in Table 4) whose pole locations are shown in Fig. 3. The geodetic results almost coincide with each other and are uniformly smaller than the NUVEL1A predictions averaged over the past 3 million years (see Fig. 4). For instance, the present-day half-spreading rate between Africa and South America at 31.1°S that is  $16.0 \pm 0.9$  mm/year, 1.2 mm/year slower than the NUVEL1A prediction, and more than 5.0 mm/year slower than the average rates over the past 80 My (Sliver et al., 1998), which shows that spreading motion of Africa–South America plate has slowed down in the last 3 million years.

**Table 1** The velocity field of geodetic stations in ITRF2000 and residuals relative to the South American plate (SA) and Africa plate (AF) (mm/year)

Site	Lon (°)	Lat (°)	Ve	Vn	$\sigma_{ve}$	$\sigma_{vn}$	Ve	Vn
			In ITRF2000				Residuals relative to SA	
South American plate								
FORT	321.6	-3.9	-4.3	12.2	0.6	0.3	-0.2	0.9
BRAZ	312.2	-15.9	-3.9	12.4	2.3	0.7	-0.3	1.0
PARA	310.8	-25.4	-1.8	12.3	5.0	2.0	1.3	0.9
KOUR	307.2	5.3	-4.5	12.0	1.0	0.3	-0.3	0.7
LPGS	302.1	-34.9	-1.7	11.4	1.0	0.4	-0.1	0.3
CORD	295.6	-31.5	-2.1	10.4	1.5	0.7	-0.8	-0.3
AREQ	288.6	-16.5	10.9	14.5	0.4	0.2	13.2	4.4
RIOG	292.3	-53.8	3.4	11.7	1.0	0.2	1.9	1.3
SANT	289.4	-33.2	18.9	16.3	0.6	0.2	19.4	6.1
MANA	300.0	-3.1	-0.6	13.9	22.1	2.7	3.2	2.9
IMPZ	312.5	-5.5	-6.4	16.4	26.3	4.3	-2.5	5.0
BOMJ	316.6	-13.3	-6.8	14.1	13.6	3.9	-2.9	2.6
CUIB	304.0	-15.6	-2.9	12.5	14.5	3.2	0.3	1.3
VICO	317.2	-20.8	-6.1	13.1	14.6	6.0	-2.3	1.6
UEPP	308.6	-22.1	-3.9	13.4	11.4	3.7	-0.8	2.0
IGM0	301.6	-34.6	3.8	17.4	28.2	9.9	5.4	6.3
VBCA	297.8	-38.7	1.9	24.4	26.2	9.0	2.7	13.6
ASC1	345.6	-8.0	-5.3	9.9	1.1	0.6	-0.6	-0.1
In ITRF2000								
Residuals relative to AF								
African plate								
LAMP	12.6	35.5	21.2	16.9	0.5	0.1	0.5	-2.2
NOTO	15.0	36.9	21.3	18.0	0.1	0.1	0.4	-1.0
NKLG	9.7	0.4	14.9	17.7	2.0	1.3	-8.4	-1.5
SUTH	20.8	-32.4	16.4	18.9	0.3	2.6	-0.2	0.4
HART	27.7	-25.9	18.1	17.9	0.0	0.6	0.6	0.2
HELW	31.3	29.9	21.3	21.0	0.3	0.1	-3.4	3.9
SIMO	34.2	18.4	16.0	17.0	1.0	0.6	-9.2	0.3
MALI	40.2	-3.0	21.0	17.1	0.1	0.5	-1.7	1.6
SEY1	55.5	-4.7	31.0	12.5	0.4	1.4	9.0	0.6
TGCV	16.8	23.0	18.0	14.5	1.2	0.6	-5.1	-4.3
GOUG	350.2	-40.3	20.2	18.5	2.4	4.9	-0.5	-0.3
YKRO	354.8	6.9	24.8	20.4	1.2	1.0	2.0	1.3
MASP	344.4	27.8	16.7	16.7	0.5	0.2	-0.9	-1.6

Figure 5 shows spreading rates of Africa–South America at 20°S in the last 35 Ma (Million years ago). The vertical lines show the uncertainty (one standard deviation). The solid triangles stand for the magnetic reconstruction results (Silver et al. 1998; Livermore et al., 1983; Gordon and Jurdy 1986). The dashed line is the unweighted least squares fit through all data. From the entire spreading histories of the South mid-Atlantic Ridge over the past 35 My, the spreading motion of the south Atlantic Ridge has been slowing down and decreased abruptly from 5 Ma, going

from a value of about 38 mm/year before 5 My to about 32 mm/year at present. In addition, our geodetic results are further compared with Sella et al. (2002), NUVEL-1A and interval spreading rates from Cande and Kent (1992). Figure 6 is a comparison of South America–Africa spreading rates at 28°S in the last 25 Ma (shaded area shows one standard deviation). It has shown a remarkable agreement between the geodetic data rates (this study and Sella et al. 2002) and a longer term trend of deceleration spreading of the south Atlantic Ridge over the past 25 My.

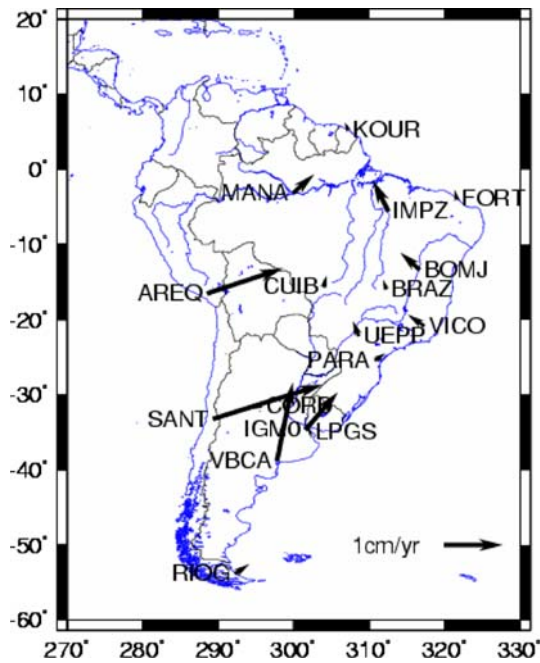


Fig. 1 Residual velocities of stations on the South American plate with respect to the South American plate

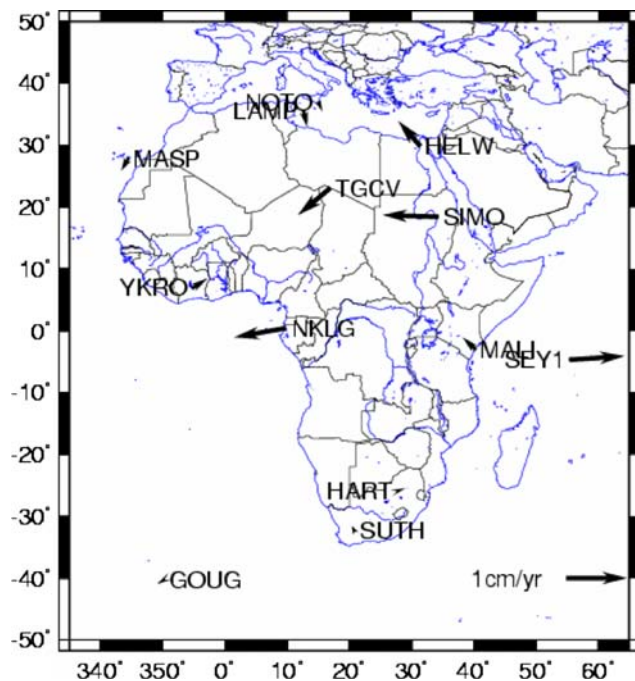


Fig. 2 Residual velocities of stations on the African plate with respect to the African plate

**Discussions**

Herein, we have presented a new method to select rigid geodetic sites that contain all of the core sites on the African and South American plates employed by

ITRF2000 for ITRF2000 orientation, that are also consistent with rigid plate motion. Therefore, this method has important applications for selecting rigid sites to establish the international terrestrial reference frame and plate motion model.

The Present-day spreading rates of Africa–South America plate were obtained from the recent 20 years of space geodetic data. Provided the South mid-Atlantic ridge spreading maintained the current average speed of 30 mm/year, the Atlantic Ocean came into being and began to spread from the Permian period or even earlier. However, according to the geological data, the Atlantic Ocean did not exist in the Permian period. Therefore we have reasons to suppose that during a certain period of geological time, the spreading rate of the mid-Atlantic ridge may have been several times greater than the current rate (Jin and Zhu 2002), which can be explicitly seen from Figs. 5 and 6. In addition, the Present-day spreading rates of Africa–South America plate are systematically slower than the NUVEL1A predictions. Comparing motion histories of Africa–South America with a new plate reconstruction shows the spreading motion of Africa–South America has decelerated by 8–15% since 35 Ma, indicating that the motion trend of Africa–South America is slowing down.

The most significant tectonic changes at the Africa–South America plate boundaries in the past 35 My are the growth of greatly thickened crust. The decelerating spreading is due to the difficulty of extruding buoyant continental lithosphere (Molnar et al. 1993). On the other hand, the younger lithosphere is warmer and more buoyant than older lithosphere, so the force due to negative buoyancy decreases for the younger extruding lithosphere. For example, westward motion of South America relative to the Atlantic Ridge causes the mean age of the extruding South America lithosphere to decrease with time, decreasing slab pull, and perhaps slowing Africa–South America spreading.

Slowing down divergence of Africa–South America since 35 Ma could be related to the same process. Perhaps the rapid continental extrusion cools sub-lithosphere mantle, increasing its strength and resistance to extrusion. Another important effect could be the increased drag between extrusion and overriding plates as the leading edge of South America and Africa thickens, possibly enhanced by “flat slab” extrusion. While all mountain belts are growth-limited by surficial and crustal processes (erosion, lateral spreading of over-thickened crust) perhaps Andean mountain belts, which may owe their initiation to rapid subduction of oceanic lithosphere, are fundamentally limited by feedback slowing of subduction; the process contains the seeds of its own demise (Norabuena et al. 1999).

The tectonic motion changes at active plate boundaries correlate with the mutual process of tectonic plates,

**Table 2** The rejecting process of sites for the South American plate

Circle	1	2	3	4	5
Total sites	18	10	7	6	5
$\Omega_x$	$-0.0288 \pm 0.0041$	$-0.0196 \pm 0.0022$	$-0.0124 \pm 0.0013$	$-0.0150 \pm 0.0013$	$-0.0180 \pm 0.0013$
$\Omega_y$	$-0.0128 \pm 0.0066$	$-0.0068 \pm 0.0035$	$0.0022 \pm 0.0016$	$0.0070 \pm 0.0012$	$0.0106 \pm 0.0011$
$\Omega_z$	$0.0283 \pm 0.0021$	$0.0417 \pm 0.0014$	$0.0128 \pm 0.0007$	$0.0128 \pm 0.0007$	$0.0113 \pm 0.0006$
$\sigma$ (mm/year)	5.8834	3.6503	1.3261	1.3192	1.2910
Sites kicked-out	8	3	1	1	0

**Table 3** The selected sites on the South American plate

Site	Lon (deg)	Lat (deg)	Vn	Ve	Residual (mm/year)			Uncertainty	
					Vn	Ve	V	$\sigma v_n$	$\sigma v_e$
FORT	321.6	-3.9	12.2	-4.3	0.2401	0.0511	0.2455	0.6	0.3
BRAZ	312.2	-15.9	12.4	-3.9	0.3704	0.0478	0.3735	2.3	0.7
KOUR	307.2	5.3	12.0	-4.5	0.0652	-0.1045	0.1232	1.0	0.3
LPGS	302.1	-34.9	11.4	-1.7	-0.3445	0.2742	0.4403	1.0	0.4
ASC1	345.6	-8.0	9.9	-5.3	-0.4524	-0.2201	0.5031	1.1	0.6

**Table 4** Relative angular velocities of Africa–South American plate

$\Omega^a$	$\lambda^a$ (°)	$\varphi^a$ (°)	$\sigma_{maj}^b$	$\sigma_{min}^b$	$\zeta^c$ (deg)	$\sigma_\Omega$	Model	References
0.279	137.2	-60.8	2.8	1.0	-4	0.006	-	This study
0.277	138.0	-62.7	3.1	1.3	-2	0.006	REVEL	Sella et al. (2002)
0.273	139.7	-61.5	8.3	3.3	-10	0.005	DEOS2k	Fernandes et al. (2003)
0.310	140.6	-62.5	2.6	0.8	-11	0.010	NUVEL-1A	DeMets et al. (1990, 1994)

<sup>a</sup> Euler rotation parameter of plate rotation,  $\Omega$  is the rotating rate (°/My),  $\lambda$  and  $\varphi$  are the longitude and latitude of rotation pole, respectively

<sup>b</sup> Two dimensional 1-sigma lengths in the degrees of the semimajor  $\sigma_{maj}$  and semiminor  $\sigma_{min}$  axes of the pole error ellipse

<sup>c</sup> The parameter  $\zeta$  is the azimuth of the semimajor ellipse axis in degrees clockwise from the North

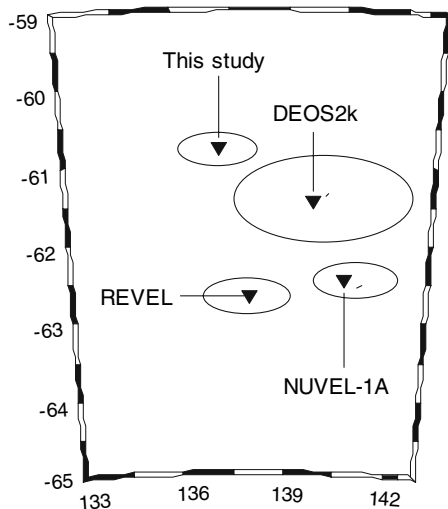


**Fig. 3** Geodetic and geological Euler's pole locations derived from this and previous studies

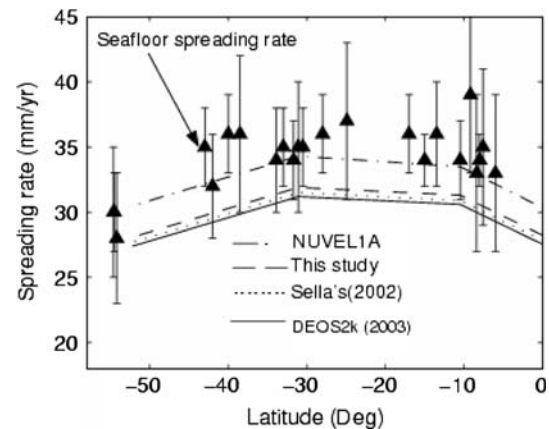


**Fig. 4** Comparison of spreading rates of Africa–South America plate

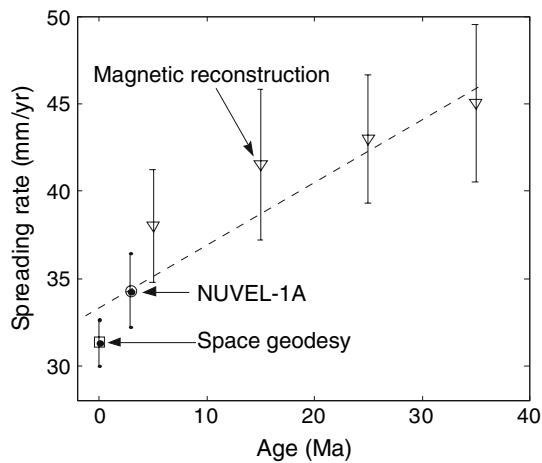


**Fig. 5** Plate motion rates of Africa–South America at 20°S in the last 35 Ma (million years ago). The vertical lines show the uncertainty (one standard deviation), the solid triangles from magnetic reconstruction (Silver et al. 1998; Livermore et al. 1983; Gordon and Jurdy 1986), and the dashed line is unweighted least squares fit through all data

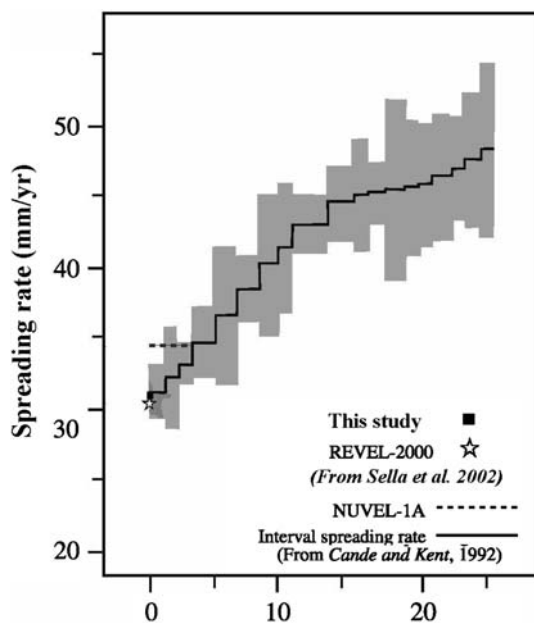


**Fig. 6** Comparison of South America–Africa spreading rates of this study at 28°S in the last 25 Ma with Sella et al. (2002), NUVEL-1A and interval spreading rates from Cande and Kent (1992) (shaded area shows one standard deviation)

therefore it is significant to solve for the divergent or convergent histories of adjacent plates. Because the Earth is continuously moving and evolving and the process is very complicated, the higher-accuracy analysis of motion trend and evolution histories of the Earth depends on the further improvement in magnetic anomalies with a high resolution and the further improvement in space techniques, longer observation time span and much wider and

more average distributions of observation sites, so as to better understand evolution histories and tectonic motion rules of the Earth.

## References

- Altamimi Z, Boucher C, Sillard P (2002) ITRF2000: a new release of the international terrestrial reference frame for earth science applications. *J Geophys Res* 107(B10):2214. doi:10.1029/2001JB000561
- Argus DF, Gordon RG (1998) Test of the rigid-plate hypothesis and bounds on intraplate deformation using geodetic data from very long baseline interferometry. *J Geophys Res* 101(B6):13555–13572
- Argus DF, Jordan TH (1991) No-net-rotation model of current plate velocities incorporating plate motion model NUVEL1. *Geophys Res Lett* 18(11):2039–2042
- Cande SC, Kent DV (1992) A new geomagnetic polarity timescale for the Late Cretaceous and Cenozoic. *J Geophys Res* 97:13917–13951
- Chu DH, Gordon RG (1999) Evidence for motion between Nubia and Somalia along the Southwest Indian Ridge. *Nature* 398(672):64–67
- DeMets C, Argus DF, Gordon RG (1990) Current plate motions. *Geophys J Int* 101:425–478
- DeMets C, Gordon RG, Argus DF (1994) Effect of recent revisions to the geomagnetic reversal time scale on estimates of current plate motions. *Geophys Res Lett* (21):2191–2194
- Fernandes RMS, Ambrosius BA, Noomen R, Bastos L, Wortel MJ, Spakman W, Govers R (2003) The relative motion between Africa and Eurasia as derived from ITRF2000 and GPS data. *Geophys Res Lett* 30(16):1828. doi: 10.1029/2003GL017089
- Fernandes RMS, Ambrosius BA, Noomen R, Bastos L, Combrinck L, Miranda JM, Spakman W (2004) Angular velocities of Nubia and Somalia from continuous GPS data: implications on present-day relative kinematics. *Earth Planet Sci Lett* (in press)
- Gordon RG, Jurdy DM (1986) Cenozoic global plate motions. *J Geophys Res* 91:12389–12406
- Gordon RG, Stein S (1992) Global tectonics and space geodesy. *Science* 256:333–342
- Heki K (1996) Horizontal and vertical crustal movements from three-dimensional very long baseline interferometry kinematic reference frame: implication for the reversal timescale revision. *J Geophys Res* 101:3187–3198
- Jin SG (2003c) Global plate tectonic motions from GPS measurements. Ph.D dissertation, Shanghai Observatory, Chinese Academy of Sciences
- Jin SG, Zhu W (2002) Present-day spreading motion of mid-Atlantic ridge. *Chin Sci Bull* 47(18):1551–1555
- Jin SG, Zhu WY (2003a) Active motion of tectonic blocks in East Asia: evidence from GPS measurement. *Acta Geol Sin Engl Ed* 77(1):59–63
- Jin SG, Zhu WY (2003b) A quantitative analysis of the global tectonic asymmetry. *Chin Astron Astrophys* 27(3):348–356
- Jin SG, Zhu WY (2004) A revision of the parameters of the NNR-NUVEL1A plate velocity model. *J Geodyn* 38(1):85–89
- Li JL, Zhang B, Wang GL (2001) A statistic of on-plate site based on a VLBI global solution. *Earth Planet Space* 53:1111–1119
- Livermore RA, Vine FJ, Smith AG (1983) Plate motion and geomagnetic field-1. Quaternary and late Tertiary. *Geophys J R Astr Soc* 73:153–171
- Molnar P, England P, Martinod J (1993) Mantle dynamics, uplift of the Tibetan plateau, and the India monsoon. *Rev Geophys Space Phys* 31:357–396

- Norabuena EO, Dixon TH, Stein S, Harrison CG (1999) Decelerating Nazca-South America and Nazca-Pacific plate motion. *Geophys Res Lett* 26(22):3405–3408
- Sella GF, Dixon TH, Mao A (2002) REVEL: a model for recent plate velocities from space geodesy. *J Geophys Res* 107(B4):ETG11–1–32
- Sillard P, Altamimi Z, Boucher C (1998) The ITRF96 realization and its associated velocity field. *Geophys Res Lett* 25(17):3223–3226
- Silver GP, Russo RM, Carolina LB (1998) Coupling of South American and African plate motion and plate deformation. *Science* 279:60–63